2

Determining the Viscosity of a Carbon Paste Used in Smelting

Preface

In the following case study, the slow viscous flow of blocks of "carbon paste" is analysed. The paste blocks are essential components of an electric smelting process by which a variety of ferro-alloys and other substances are produced. The problem is first proposed in its most general form. A nondimensionalisation using typical parameter values of the process then shows that a much simpler set of equations may be used to analyse the flow After examining the qualitative details of the fluid motion in various key regions of the flow, an asymptotic analysis of a long thin block of paste allows us to develop a good general understanding of the main principles of slow viscous flow in paste blocks The theory highlights the key differences between various tests that are used to determine the viscosity of carbon paste. Finally, some fairly straightforward numerical analysis is used to show that the general problem is amenable to simple methods; the numerical results also show that in many cases the "long thin" analysis used earlier can produce remarkably accurate results.

The work outlined below is part of research that was produced during and after the 1988 European Study Group with Industry, which was held at the University of Heriot-Watt, Scotland. Some extensions to the work presented here are suggested as projects for the interested student in section 2.6. Close links have continued to be maintained between industrial mathematicians and the ELKEM ASA, the Norwegian company that originally proposed the problem. A number of other problems (see [1], [4], and [3]) concerning various aspects of the electric smelting industry have also been considered in detail and have led to some interesting mathematical problems.

2.1 Continuous Electrode Smelting

Electric smelting is a popular process for producing a variety of materials such as ferro-alloys, silicon, and calcium carbide. Heat is provided for the

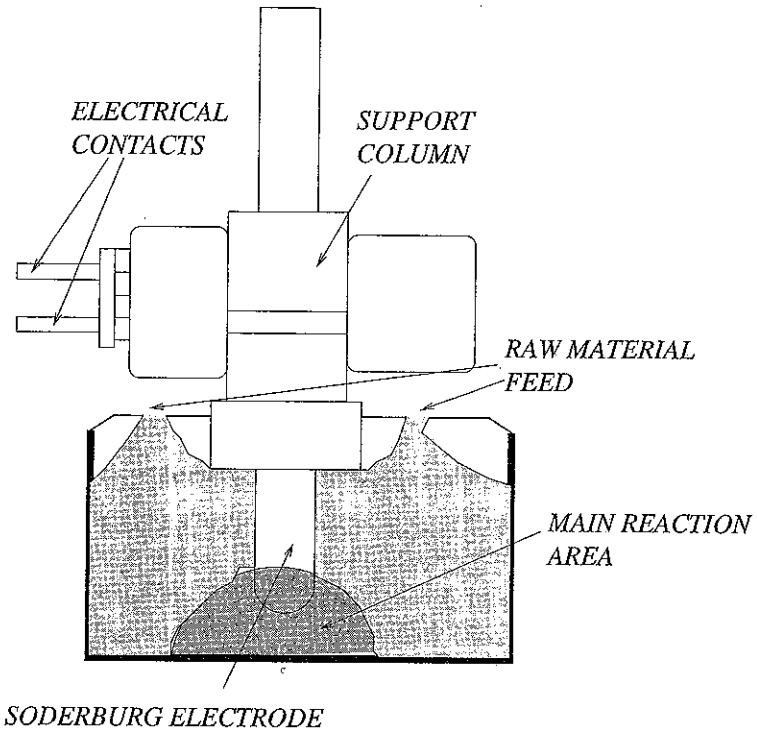

Fig. 2.1 Schematic diagram of carbon electrode furnace

smelting furnace via substantial (up to 150,000 Amps) electrical currents that are passed to the heart of the furnace through a carbon electrode. Figure 2.1 gives the schematic details of the physical arrangement.

As the smelting takes place, the electrode is consumed (depletion rates of 1m per day are typical) and must be replenished A practical way of achieving this is to produce a continuous carbon electrode immediately above the furnace. This is normally done by feeding cylinders of carbon "paste" into the centre of a cylindrical steel casing (diameter 1–2 m) which is gradually heated. As the paste warms, it flows to fill the cylinder and is eventually "baked" solid at around 500°C in the region where the current enters the electrode. Baking improves both the strength and electrical conductivity of the electrode, and is essential for satisfactory current transfer. Electrodes of this type have come to be called Søderburg electrodes after the Norwegian who pioneered their development in the early part of this century.

To design an efficient Søderburg electrode, the viscosity of the carbon "paste" must be known, and this will be the main question that concerns us here. Traditionally at the smelting factory a number of simple experiments

have been carried out to determine the viscosity These will be considered more in detail later, but basically they involve taking a cube or cylinder of the heated carbon paste and simply letting it "slump" under its own weight. Measurements of the bulge at the base of the sample are made, and the viscosity is inferred from the growth of the bulge with time. The industrial practitioners specifically want to know:

- Which sort of viscosity test is likely to provide the most reliable answers?
- What size and geometry of paste sample will give the most accurate results without taking too much time to test?
- How does the prospective duration of each test depend on the physical parameters?
- What sort of errors may the experiments be expected to produce?

Before we can answer any of these questions, the nature of the carbon paste itself must be understood. The paste is not a simple one-component fluid, but consists of a binder (normally pitch or tar) into which is mixed particles of calcined anthracite (coke). The particles may have diameters ranging from 125 μm to 15 mm, and the particle size range may be varied to produce electrodes with different electrical, thermal, and strength properties Experience has shown, however, that to all intents and purposes the paste may be taken to behave as a single viscous fluid. It is worth mentioning that there *are* circumstances for which this is not true, as the paste may "segregate" in the electrode. During segregation the particles clump together and large regions of the paste consist only of binder. Though this may cause severe problems during the smelting process, it is not our concern here; for more details concerning this interesting subproblem, the reader is referred to [1]. Regarding the thermal properties of the paste (which is solid at room temperature), experiments have shown that, at 50–80°C softening takes place and flow occurs. When the viscosity is being measured experimentally, tests are carried out at a constant temperature. This is convenient for our purposes, since it means that the thermal properties of the paste need enter into the problem only as parameters.

As far as the viscosity experiments are concerned, there are three recognised ways of causing a heated sample to "bulge" to allow a viscosity measurement to be made. These are:

(1) The "plasticity" test: a sample of paste is heated to around 300°C, placed on a rigid impermeable surface, and allowed to slump under its own weight

(2) The "velocity test": a metal plate is applied to the top (planar) surface of the sample and forced to move downwards with a (normally constant) prescribed velocity

(3) The "viscometer": identical to the velocity test except that a constant force is used.

The terminology is used in deference to that standard in the industry In fact all three tests are really viscometers, and no plastic flow in the normal solid-mechanics sense of the word occurs in the plasticity test. It is also worth noting that the velocity test and the viscometer test generally take much less time to complete than the plasticity test.

2.2 Problem Formulation

We fix our ideas by considering a block of paste occupying a region D which is initially rectangular with height h and semiwidth L. As shown in figure 2.2, the top surface of the sample is denoted by S_T, the surface in contact with the rigid plane at $y = 0$ by S_B and the (initially vertical) sides of the sample by S_- and S_+.

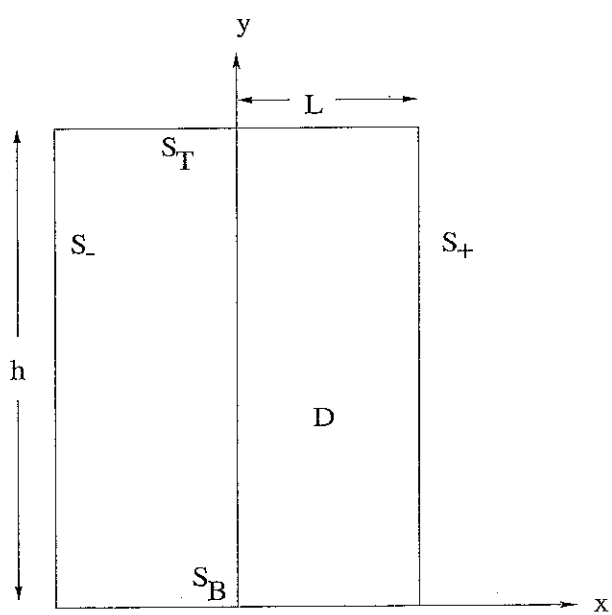

Fig 2.2. Geometry and nomenclature of paste block

The first priority in the analysis of the problem is to determine which parameters are important and which effects dominate, and we tackle this by nondimensionalising. We carry this out by scaling lengths with h (thus tacitly assuming that the paste block has an aspect ratio of order 1), the fluid velocity $\boldsymbol{q}$ with U_∞ where U_∞ is a representative speed (for example the average speed of the centre of the top of the sample), the time t with a representative time τ, and the pressure p and the stress tensor $\boldsymbol{T}$ with $\mu U_\infty/h$, where μ is the dynamic viscosity (to be determined). The Navier–Stokes equations (see, for example [7]) with a gravity body force then become, in nondimensional variables,

$$\mathrm{Re}[\mathrm{St}^{-1}\boldsymbol{q}_t + (\boldsymbol{q} \cdot \nabla)\boldsymbol{q}] = -\nabla p + \nabla^2 \boldsymbol{q} - (\mathrm{Re}/\mathrm{Fr})\boldsymbol{j},$$
$$\nabla \cdot \boldsymbol{q} = 0,$$

where $\boldsymbol{j}$ denotes the unit vector in the y direction. Here the subscripts denote differentiation, and as usual the Reynolds, Froude, and Strouhal numbers are defined by

$$\mathrm{Re} = \frac{hU_\infty \rho}{\mu}, \qquad \mathrm{Fr} = \frac{U_\infty^2}{gh}, \qquad \mathrm{St} = \frac{\tau U_\infty}{h},$$

where ρ denotes the fluid density (assumed known).

We must now consider the relative sizes of these parameters. Since none of the tests involves impulsive loading, we assume that the Strouhal number is of order one, so that $U_\infty \sim h/\tau$. Using representative values of $h \sim 1$ m, $U_\infty \sim 1$ m/h, $\rho \sim 3000$ kg/m^3, and assuming that the viscosity is of order of magnitude 10^8 Pa sec (although the paste viscosity may vary by orders of magnitude, the representatives from the factory assured us that this was a typical viscosity value), we find that

$$\mathrm{Re} = O(10^{-8}), \qquad \mathrm{Fr} = O(10^{-8}).$$

To lowest order, the nondimensional equations of motion become

$$\nabla p = \nabla^2 \boldsymbol{q} - \alpha \boldsymbol{j} \tag{2.1}$$
$$\nabla \cdot \boldsymbol{q} = 0, \tag{2.2}$$

where $\alpha = \mathrm{Re}/\mathrm{Fr}$. Already, the formidable problem posed by the Navier–Stokes equations has been greatly simplified; to a good order of approximation, the correct equations are simply the slow flow equations with a body force. The problem must be completed by the specification of suitable initial and boundary conditions. Assuming that the shape of the paste block is specified at $t = 0$, we have the standard no-slip viscous boundary condition

on $y = 0$, the sides S_+ and S_- are stress-free, and the boundary conditions that must be applied on the top surface S_T depend on which test we are using.

The equations of motion (2 1) and (2.2) hold for arbitrary paste blocks, but may be further simplified if the pressure is eliminated and we work only in *two dimensions*. Taking the curl of (2 1) and defining a stream function $\psi(x, y)$ so that $u = \psi_y$ and $v = -\psi_x$, the full problem becomes

$$\nabla^4 \psi = 0 \quad ((x, y) \in D),$$
$$\psi = \psi_y = 0 \quad ((x, y) \in S_B),$$
$$\boldsymbol{T} \cdot \boldsymbol{n} = 0 \quad ((x, y) \in S_+ \cup S_-),$$
$$(D/Dt)[x - \xi(y, t)] = 0 \quad ((x, y) \in S_+ \cup S_-), \tag{2 3}$$

$$\left.\begin{array}{lll} \boldsymbol{T} \cdot \boldsymbol{n} = 0 & & \text{(plasticity test)} \\ \psi_y = 0 & \psi_x = \dot{s}(t) & \text{(velocity test)} \\ \psi_y = 0 & -p - \psi_{xy} = \gamma(t) & \text{(viscometer)} \end{array}\right\} \quad ((x, y) \in S_T).$$

Here $D/Dt = \partial/\partial t + (\boldsymbol{q} \cdot \nabla)$ denotes the standard convective derivative, $\boldsymbol{n}$ is the unit normal to the boundary, and $\dot{s}(t)$ and $\gamma(t)$ denote a nondimensional speed and normal stress respectively. The boundary of the sample is denoted by $x = \xi(y, t)$. As usual in slow flow problems, time enters into the problem only as a parameter and via the boundary conditions; the body force enters only via the pressure p in the boundary conditions.

2.3 Simplified Analysis

The full problem in the previous section is too complicated to solve in closed form, and a numerical solution is required. For the reasons explained above, however, we first search for some simplified versions of the problem where theoretical progress may be made.

2.3.1 Corner Solutions

First, we consider the general form of solutions near to a corner Although such local analysis is unlikely to answer any of the industrialist's questions directly, at this stage any information on the nature of the flow is helpful. Each test may be examined, but, confining ourselves to the plasticity test and leaving the other cases as exercises for the interested student, it is easy to show that the local behaviour of solutions may be determined by simple separation of variables. Using x and y to denote local coordinates,

we find that:

(i) near a top corner (where two stress-free surfaces meet),

$$u \sim -\frac{1}{4}\alpha xy, \quad v \sim \frac{1}{8}\alpha(x^2+y^2), \quad p \sim -\frac{1}{2}\alpha y,$$

(ii) near the line of symmetry at the top,

$$u \sim \alpha\beta xy, \quad v \sim -\frac{1}{2}\alpha\beta(x^2+y^2), \quad p \sim \alpha(-1-2\beta)y,$$

where β is an arbitrary constant that would have to be determined by a matching procedure (see, for example [6])

(iii) near a bottom corner (where a stress free surface meets a fixed surface),

$$u \sim -\frac{1}{3}\alpha xy, \quad v \sim \frac{1}{6}\alpha y^2, \quad p \sim -\frac{2}{3}\alpha y,$$

(iv) near the bottom line of symmetry,

$$u \sim \alpha\delta xy, \quad v \sim -\frac{1}{2}\alpha\delta y^2, \quad p \sim \alpha(-1-\delta)y,$$

where δ is arbitrary. Although these expressions for u, v, and p may easily be verified to be solutions to the local problem, evidently they all have the property that $u = 0$ at $x = 0$, and thus predict no bulging of the sample. To produce the required outward movement of the walls of the sample, it is necessary to recognise that the flow is dominated by an eigensolution. The eigenproblem is simple to pose: near the bottom left-hand corner, for example, employing local polar coordinates, the equation of motion is

$$\nabla^4\psi = 0 \quad (r \geq 0,\ 0 \leq \theta \leq \pi/2),$$

while the boundary conditions are the no-slip conditions

$$\psi_r = \psi_\theta = 0 \quad (\theta = 0)$$

and the zero-stress conditions on the free boundary $\theta = \pi/2$. To express these in a convenient form, we note that the stress tensor is given (in dimensional variables) by

$$\boldsymbol{T} = \begin{pmatrix} -p + 2\mu u_x & \mu(u_y + v_x) \\ \mu(u_y + v_x) & -p + 2\mu v_y \end{pmatrix},$$

and since the outward normal to the free boundary is given by $\boldsymbol{n} = (-1, 0)$, the stress-free condition amounts to (returning to nondimensional variables)

$$-p + 2u_x = u_y + v_x = 0 \quad (\theta = \pi/2).$$

The second condition may easily be transformed to polar coordinates to give

$$r^2\psi_{rr} - r\psi_r - \psi_{\theta\theta} = 0,$$

while the first may be dealt with by differentiating with respect to y and using the y-momentum equation to eliminate the term p_y. This finally leads to

$$\psi_{\theta\theta\theta} - 3r\psi_{r\theta} + 4\psi_\theta + 3r^2\psi_{rr\theta} = 0 \quad (\theta = \pi/2),$$

which is the final boundary condition for the homogeneous problem.

Having posed the problem for the bottom corner, the top corner may be examined in a similar way, giving the problem

$$\nabla^4\psi = 0 \quad (r \geq 0,\ -\pi/2 \leq \theta \leq 0),$$

$$\left.\begin{aligned} r^2\psi_{rr} - r\psi_r - \psi_{\theta\theta} &= 0 \\ \psi_{\theta\theta\theta} - 3r\psi_{r\theta} + 4\psi_\theta + 3r^2\psi_{rr\theta} &= 0 \end{aligned}\right\} \quad (\theta = -\pi/2 \text{ and } \theta = 0),$$

Both problems may be solved by standard separation of variables, or more simply by seeking a solution of the form

$$\psi = r^\lambda[A\cos\lambda\theta + B\sin\lambda\theta + C\cos(\lambda-2)\theta + D\sin(\lambda-2)\theta],$$

where λ, A, B, C, and D are constants. Imposing the boundary conditions, we find that for the bottom corner either $\lambda = 1$ (giving again that u is zero along $\theta = \pi/2$) or λ must satisfy the equation

$$\tan^2(\pi\lambda/2) = (\lambda-1)^2/\lambda(2-\lambda) \tag{2.4}$$

It may easily be shown that (2.4) has precisely two real solutions $\lambda \sim 0.405$ (which must be rejected since it leads to singular behaviour for u at $r = 0$) and $\lambda \sim 1\ 595$. Thus an eigensolution with a velocity

$$\psi_r \sim r^{0.6}$$

along $\theta = \pi/2$ is possible. This suggests that the bulging that takes place in the plasticity test is associated with a free boundary that grows like $tr^{0.6}$. Near to the top corner, λ must satisfy

$$\tan^2(\pi\lambda/2) = \lambda(\lambda-2)/(1-\lambda)^2, \tag{2.5}$$

an equation whose only real zeros are 0, 1, and 2. All three of these solutions give $u = 0$ on $\theta = -\pi/2$ and therefore do not allow bulging. (It is worth pointing out that (2.4) and (2.5) possess infinitely many complex solutions as well as the real ones discussed above. These have not been investigated,

but almost certainly correspond to the classical "Moffatt vortex" solutions (see for example [5]) that are typical in slow flow problems).

The conclusions of our local analysis may be summarised as follows.

(i) The behaviour at the corners is dominated by eigensolutions.

(ii) With or without eigensolutions, the bottom corner point cannot move. This is essentially a consequence of the no-slip condition and is in direct contrast to the inviscid case. (For analysis of the inviscid case see [8].)

(iii) When eigensolutions are included, bulging can take place at the bottom of the sample but not at the top

2.4 Special Geometries

Even the simple corner solutions examined in the previous section have allowed us to begin to piece together what happens to a sample of paste during testing. The top surface initially remains much as it began, and most of the movement occurs at the bottom of the sample, since bulging occurs at the corners. To further analyse the process, we consider some special geometries. Though it is tempting to examine the case of a "short fat lump of paste", it may easily be shown that little of value can be wrung from this case. Though the geometry leads to some simplifications, it is clear from the outset that there will be boundary layers at the edges of the sample, and these are precisely the regions that interest us most. Analysis of the boundary layers involves consideration of the original full problem, and thus little progress may be made.

The prognosis is altogether more encouraging if we consider the other obvious limit of a tall thin sample of paste. Assuming that $L/h = \epsilon \ll 1$, we consider the region $x > 0$ for simplicity and impose symmetry conditions on $x = 0$ (which will subsequently be denoted by S_A). Making the obvious scalings $x = \epsilon X$, $u = \epsilon U$, and $\xi = \epsilon\eta$, the scaled nondimensional problem becomes

$$p_X = U_{XX} + \epsilon^2 U_{yy}, \tag{2.6}$$

$$\epsilon^2 p_y = v_{XX} + \epsilon^2 u_{yy} - \epsilon^2\alpha, \tag{2.7}$$

$$U_X + v_y = 0. \tag{2.8}$$

Assuming that $U = U_0 + \epsilon U_1 + \epsilon^2 U_2 + \cdots$ and using similar expansions for v, p, and η, a regular perturbation solution of (2.6)–(2.8) that additionally satisfies the symmetry conditions $U = v_X = 0$ on $X = 0$ may easily be

determined. Correct to order ϵ^2, we find that

$$U = -Xv_{0y} - \epsilon X v_{1y} + \epsilon^2\left[-\frac{1}{6}X^3(-2v_{0yyy} + g_{0yy}) - Xq_y\right],$$

$$v = v_0(y,t) - \epsilon v_1(y,t) + \epsilon^2\left[\frac{1}{2}X^2(g_{0y} + \alpha - 2v_{0yy}) + q(y,t)\right],$$

$$p = -(v_{0y} + g_0) + \epsilon(-v_{1y} + g_1) + \epsilon^2\left[\frac{1}{2}X^2(v_{0yyy} - g_{0yy}) + g_2(y,t)\right],$$

where the functions q, g_1, g_2, and g_3 remain to be determined. Imposing the free surface kinematic boundary condition gives

$$(\eta_0)_t + (\eta_0 v_0)_y = 0 \tag{2.9}$$

to leading order, and another equation relating v_0 and η_0 may be determined by imposing the stress-free conditions on $X = \eta(y,t)$. There are two components of $\boldsymbol{T}\cdot\boldsymbol{n}$ that must be zero; the x component gives

$$-g_0 + v_{0y} = -g_1 - v_{1y} = 0$$

correct to $O(\epsilon)$, while the $O(\epsilon^2)$ contribution relates the functions q, g_2, and g_3. The y component yields nothing until we reach the $O(\epsilon^2)$ terms, whereupon we find that

$$4(\eta_0 v_{0y})_y = \alpha\eta_0 \tag{2.10}$$

The leading-order solution thus becomes

$$U = -Xv_{0y} - \epsilon X v_{1y} + \epsilon^2\left[\frac{1}{2}X^3(v_{0yyy} - Xq_y\right],$$

$$v = v_0 - \epsilon v_1 + \epsilon^2\left[\frac{1}{2}X^2(\alpha - 3v_{0yy}) + q\right],$$

$$p = -2v_{0y} - 2\epsilon v_{1y} + \epsilon^2\left[X^2 v_{0yyy} + g_2\right],$$

where η_0 and v_0 are determined by (2.9) and (2.10). As far as boundary and initial conditions for the equations for η_0 and v_0 are concerned, clearly it makes sense to specify an initial condition for η_0. Also, since (2.10) is of second order in y, we expect to be able to satisfy two boundary conditions. The full problem requires that two stress conditions are satisfied on the top surface of the sample, while two no-slip conditions apply to the bottom of the sample. Therefore two conditions must be dropped, and we may expect there to be boundary layers at the top and bottom of the sample. Since we want results that reflect properties of both the top and the bottom of the sample, we impose $v_0 = 0$ on $y = 0$ and one stress condition on the sample top

2.4.1 Further Analysis of the Velocity Test

Now that the framework for analysing the long thin paste block has been established, we derive some results. For the velocity test, where v is specified on the top of the sample, some progress may be made with the governing equations for the period soon after the experiment begins. Expanding v_0 and η_0 in powers of t, assuming that $v = -V_T$ on $y = 1$ and $\eta_0(y,t) = 0$ (an initially straight sided block) the solution satisfying $v_0 = 0$ on $y = 0$ is given by

$$\eta_0 = 1 + \frac{t}{8}(8V_T - 2\alpha y + \alpha) + O(t^2),$$

$$v_0 = \frac{1}{8}\alpha y^2 - y\left(V_T + \frac{\alpha}{8}\right) + \frac{t}{192}\left[\alpha y(2\alpha y^2 - 3\alpha y + \alpha - 24V_T y + 24V_T)\right] + O(t^2).$$

Three separate cases are identified (as shown in figure 2.3):

(i) For $V_T > \alpha/8$, both the top and the bottom of the sample will bulge as the top plate is pushed down. The free boundary is linear in t, and the horizontal velocity on the top and the bottom of the sample is proportional to x.

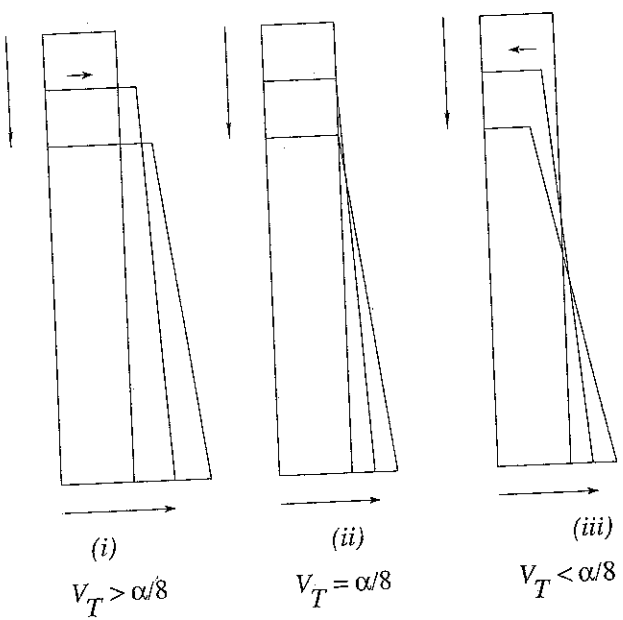

(ii) When $V_T = \alpha/8$, the imposed velocity is just large enough to ensure that $\eta_0 = 1$ at $y = 1$, so that the horizontal velocity on the top surface is zero.

(iii) When $V_T < \alpha/8$, the sample "necks" as the top surface moves towards the y axis, while the bottom surface moves away from it.

Near $y = 0$ and $y = s(t)$ the analysis is not valid, since boundary layers are present; nevertheless the outer solution may still be used to predict the viscosity from the bulging. Evaluating η_0 on $y = 0$ and restoring the dimensional variables reveals that, if the top plate moves with speed U_∞ and the maximum semiwidth of the sample at any time is BL, say, then the dynamic viscosity is given by

$$\mu = \frac{h^2\rho g t}{8(h(B-1) - U_\infty t)} \tag{2.11}$$

2.4.2 Analysis of the Viscometer Test

The only change required to examine this case for small t is to impose the boundary condition $-p_0 + 2v_{0y} = \gamma(t)$ as well as $v_0 = 0$ on $y = 0$. For a constant load $\gamma(t) = -\gamma$, say, we then easily find that

$$\eta_0 = 1 + \frac{t}{4}(\gamma - \alpha y + \alpha) + O(t^2),$$

$$v_0 = \frac{1}{8}\alpha y^2 - \frac{y}{4}(\gamma + \alpha) + \frac{t}{96}[\alpha y(\alpha y^2 - 3\alpha y + 3\alpha - 3\gamma y + 6\gamma)] + O(t^2).$$

The predicted bulge is therefore once again linear in y, though no necking of the sample can occur unless $\gamma < 0$. (Although such an experiment would be rather hard to set up, there is no reason why the viscosity could not be measured by forcing the top of the sample to rise and measuring the necking.) For a maximum sample semiwidth BL and a (dimensional) load Γ, redimensionalisation gives the result corresponding to (2.11) as

$$\mu = \frac{t(\Gamma + h\rho g)}{4(B-1)}. \tag{2.12}$$

Actually, some extra information is available here, since in this case the speed of the top of the sample is also unknown. The possibility thus arises of estimating the viscosity from the speed of the plate. Assuming that $\eta_0 = 1 + O(t)$ for $t \ll 1$ and solving (2.9) and (2.10) for small time, we find, on

imposing the conditions that $v_0 = 0$ on $y = 0$ and $-p_0 + 2v_{0y} = -\gamma$ on $y = s(t)$, that

$$v_0 = \frac{1}{8}\alpha y^2 + \frac{y}{4}[-\gamma - \alpha s(t)].$$

Insisting that $v_0 = \dot{s}$ on $y = s(t)$ thus gives an ordinary differential equation for $s(t)$, which has the solution

$$s(t) = \frac{2\gamma e^{-\gamma t/4}}{\alpha + 2\gamma - \alpha e^{-\gamma t/4}}.$$

A redimensionalisation now shows that the effective viscosity is given in terms of s by

$$\mu = \frac{\Gamma t}{4\log[(2h\Gamma + h\rho g s)/s(h\rho g + 2\Gamma)]} \sim \frac{ht(\Gamma + h\rho g/2)}{4(h - s)}.$$

2.4.3 Analysis of the Plasticity Test

The plasticity test involves a further complication: there is no reason why the top surface of the sample should remain flat. However, it is fairly easy to show that, to leading order, the top surface *does* remain parallel to the x axis Small-time expansions then show that

$$\eta_0 = 1 + \frac{t\alpha}{4}(1 - y) + \frac{\alpha t^2}{32}(-2\alpha y + \alpha y^2 - 4D) + O(t^3),$$

$$v_0 = \frac{1}{8}\alpha y^2 - \frac{\alpha y}{4} + \frac{ty}{96}[\alpha^2 - 3\alpha^2 y + \alpha^2 y^2 + 24\alpha D)] + O(t^2),$$

where D is a constant that could be obtained by going to higher order For, therefore, the viscosity may be estimated using

$$\mu = \frac{h\rho g t}{4(B - 1)} \tag{2.13}$$

2.4.4 The Boundary Layer at the Base of the Sample

The results (2.11), (2.12), and (2.13) give us our first concrete formulae, and, as we shall see later, are capable of giving accurate predictions Before proceeding, however, some account must be taken of the boundary layers at the top and bottom of the sample. Although for practical purposes it is probably not necessary to give all the details of the boundary layer problem, good mathematical practice demands that we should at least satisfy ourselves

full problem applies, and thus a numerical solution is required in general. Some progress may be made, however, with the small-time problem. Considering by way of an example the boundary layer at the base of the sample in the velocity test, we exploit the facts that the boundary S_+ remains vertical for $t \ll 1$ and the outer velocity is known to be

$$v_0 = -X\left[\frac{1}{8}\alpha y^2 + Ky\right] + O(t) \quad (K = -V_T - \alpha/8).$$

Introducing a stream function Ψ that has been scaled (in addition to y) with ϵ and further setting $\Psi = -KYX + \Phi$, the matching problem becomes, to leading order,

$$\nabla^4\Phi = 0 \qquad (0 \le X \le 1, \quad 0 \le Y < \infty)$$

with boundary conditions

$$\Phi = \Phi_{XX} \qquad (X = 0),$$

$$\Phi_{YY} - \Phi_{XX} = 0, \quad \Phi_{XXX} + 3\Phi_{XYY} = 0 \qquad (X = 1),$$

$$\Phi = 0, \quad \Phi_Y = KX \qquad (Y = 0)$$

and matching condition $\Phi \to 0$ as $Y \to \infty$. A symmetrical separation of variables solution that is suitably behaved as $Y \to \infty$ is given by

$$\Phi = \exp(-\lambda Y)[BX\cos\lambda X + C\sin\lambda X],$$

while the two conditions on $X = 1$ mean that there can only be non-trivial solutions for the constants B and C if

$$\lambda + \sin\lambda\cos\lambda = 0. \tag{2.14}$$

The expression (2.14) is familiar in both elasticity and slow viscous flow; it is the Papkovitch–Fadle equation, and many of its properties are known. In particular it possesses an infinite number of complex solutions which are given, for large k, by

$$\lambda_k = \left(k - \frac{1}{2}\right)\pi + \frac{1}{2}i\log(4k\pi) + O(\log k/k).$$

Although it is possible to completely determine the coefficients of the eigenfunction expansion so that the conditions at $Y = 0$ are satisfied, it is not a trivial matter, since the problem is a so-called "non-canonical" one. Biorthogonal functions and collocation must be used, the net result being an infinite system of linear equations for the coefficients, which may be made diagonally dominant provided sufficient care is taken. Of most importance is

the fact that, though the minutiae are complicated (see, for example [9]), the details may all be taken care of.

2.5 Numerical Analysis and Results

The analysis that was carried out on the Navier–Stokes equations allows the numerical problem for general blocks of paste to be considerably simplified. Instead of solving a fully time-dependent nonlinear problem, we now have to solve what amounts to a fourth-order linear time-independent equation of motion. The position of the free surface may then be advanced using the kinematic condition. Space does not permit any but the barest numerical details (a full discussion may be found in [2]), but essentially the most convenient way to solve the problem is to use the finite-element method to solve the partial differential equation, followed by a Lagrangian method to advance the boundary.

2.5.1 Finite-Element Method

To apply the finite-element method, the equations are most conveniently written as

$$\sigma_{11x} + \sigma_{12y} = 0, \qquad \sigma_{21x} + \sigma_{22y} = 0, \qquad u_x + v_y = 0, \tag{2.15}$$

where

$$\sigma_{11} = -p + 2u_x, \quad \sigma_{12} = \sigma_{21} = u_y + v_x, \quad \sigma_{22} = -p + 2v_y.$$

The boundary conditions are

$$u = v = 0 \ ((x, y) \in S_B), \ T_x = T_y = 0 \ ((x, y) \in S_+),$$
$$u = T_y = 0 \ ((x, y) \in S_A),$$

and, for $(x, y) \in S_T$,

$$T_x = T_y = 0 \qquad \text{plasticity test}$$
$$u = 0, \ v = \dot{s}(t) \qquad \text{velocity test}$$
$$u = 0, \ T_y = \gamma(t) \qquad \text{viscometer test,}$$

where the surface tractions T_1 and T_2 are given by

$$T_1 = \sigma_{11}\frac{\partial x}{\partial n} + \sigma_{12}\frac{\partial y}{\partial n}, \qquad T_2 = \sigma_{12}\frac{\partial x}{\partial n} + \sigma_{22}\frac{\partial y}{\partial n},$$

n being in a direction normal to the boundary. Dividing the flow region D into

are approximated by polynomials one degree higher than those used for the pressure. Using quadratic and linear polynomials respectively, we choose the coefficients of the polynomials to satisfy the weak (integrated) forms of (2.15). (Details of the numerical procedures may be found in standard text books on finite and boundary elements.) In this way the whole problem may be reduced to a system of linear equations which may then be solved by standard methods. Once the solution has been computed at a particular time, the Lagrangian equations

$$\frac{dx}{dt} = u, \quad \frac{dy}{dt} = v$$

are integrated in an explicitly discretised form to advance the boundary, whereupon the whole process begins again. The scheme constitutes a quick and accurate method of solving the full problem. Although for simplicity only two-dimensional cases are considered here, the method could also be extended to three dimensions with little extra effort.

2.5.2 Results

Numerical results are shown for a typical paste block of unit aspect ratio in figure 2.4. The calculations were performed using 100 elements (giving 231 nodes and 528 variables), and numerical tests suggested that this gave results with a relative error of about 10^{-4}. The results display qualitative features that are familiar to Elkem from their experiments: in the plasticity test there is a pronounced bulge near to the bottom of the sample, whilst the bulging is more evenly distributed along the lateral boundary of the sample in the viscometer. In both the plasticity test and the viscometer, the top edge of the boundary nearest to the free surface tends to become slightly elevated. This cannot of course happen in the velocity test, where once again the bulging seems to take place over most of the free boundary rather than in a local area. It is of interest to compare the numerically calculated results to the predictions of (2.11), (2.12), and (2.13). In all of the results given below, the paste sample had a viscosity of $\mu_p = 10^8$ Pa sec and a density of 3000 kg/m^3. The gravitational constant g was taken to be 9.8 m/s^2, the paste block was assumed to be 1 m high, and the velocity scale was taken to be 1 m/hr. For the velocity and viscometer tests, V_T and γ were both taken to be 1. Table 2.1 shows results for the paste block shown in figure 2.4. The time increment is denoted by n, which varied for different tests; this reflects the fact that each method of viscosity measurement has its own characteristic experimental time. For the results discussed below, it was found appropriate to use time increments

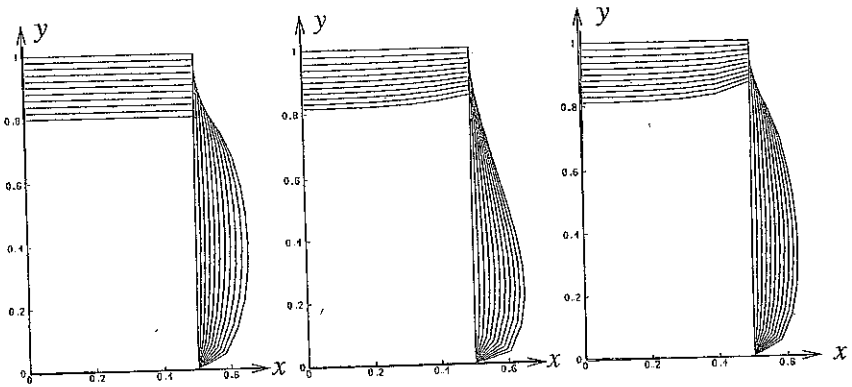

Fig. 2.4 Numerical results for paste block of unit aspect ratio (100 elements) (a) viscosity test, (b) plasticity test, (c) viscometer

Table 2.1. *Viscosity Ratios μ/μ_p Predicted by Asymptotic Model in the Case $\epsilon = 1$*

n	Velocity Test (Bl)	Plasticity Test (Bl)	Plasticity Test (Ht)	Viscometer (Bl)	Viscometer (Ht)
1	0.436	1.657	1.170	1.299	1.199
2	0.402	1 665	1 170	1 301	1 202
3	0.373	1 674	1 171	1 302	1 206
4	0.347	1.683	1.171	1.304	1.210
5	0.325	1.693	1 171	1.307	1.213
6	0.305	1 703	1 172	1.310	1.217
7	0.288	1 714	1 172	1 313	1 221
8	0.273	1 725	1 173	1 317	1 225
9	0.259	1 738	1 174	1 322	1.230
10	0.247	1.751	1 175	1.327	1.235

of 0.02 h, 0.2 h, and 0 07 h respectively for the velocity, plasticity, and viscometer tests The table gives values of μ/μ_p (which should take the value 1 if the theory is perfect) for each experiment, μ having been calculated via the formula discussed previously. Results (labelled "Ht") are also given for cases where the height of the sample is measured instead of the bulge.

Table 2.1 compares exact results with a theory that is valid in the limit $\epsilon \to 0$ for the case $\epsilon = 1$, and so one would not expect there to be any agreement. Nevertheless, all of the results indicate that the predicted viscosities are at least of the correct order of magnitude. Although the velocity test predicts viscosities that are incorrect by factors of 2–4 (depending on when

Table 2.2. *Viscosity Ratios μ/μ_p Predicted by Asymptotic Model in the Case $\epsilon = 1/10$*

n	Velocity Test (Bl)	Plasticity Test (Bl)	Plasticity Test (Ht)	Viscometer (Bl)	Viscometer (Ht)
1	0.956	1.169	1.009	1.090	1.014
2	0.829	1 166	1 016	1 091	1 023
3	0.728	1 162	1 023	1 091	1 032
4	0.646	1.159	1.029	1.091	1.041
5	0.578	1.156	1.036	1.091	1.050
6	0.521	1 153	1 042	1 091	1 058
7	0.472	1.150	1 048	1 091	1 067
8	0.430	1.148	1.053	1 091	1 075
9	0.393	1.145	1.059	1.091	1.083
10	0.361	1.143	1 064	1.090	1 091

accurate results, especially when the height of the sample is measured rather than the bulge.

Table 2.2 gives results when the aspect ratio of the sample is 10, so that the parameter $\epsilon = 0.1$ is truly small. Here we may anticipate that the theory will be much more accurate, and this expectation is borne out. Once again, the velocity test seems to be the least accurate experiment, though for small times it gives acceptable results. Each of the other tests gives results that are accurate to a few percent, though once again it seems that it is slightly better to measure the height of the sample rather than the bulge.

2.6 Final Conclusions

What has our modelling achieved? We began this study with a number of clearly specified goals, so let us review these one by one.

First, we now have a much improved physical understanding of how the process works. The type of bulging that may be expected for each test, "necking" and other effects may now all be explained in terms of a clearly defined mathematical framework.

The key nondimensional parameters have been identified: the Reynolds number is so small that inertia cannot be of any importance, and the process is driven by the parameter

$$\frac{\mathrm{Re}}{\mathrm{Fr}} = \frac{gh^2\rho}{\mu U_\infty}.$$

By investigating obvious alternative nondimensionalisations using the velocity and loading of the top plate, timescales could be determined for

each test (details left to the reader). In particular, the velocities and loadings that equalise the time taken for each experiment to be performed could be determined.

After examining the results for the tall thin paste block, the practitioner should have a good feel for how changes in the experiment are likely to be reflected in the results. Examining the general properties of the model in this simple case shows how the results are likely to change if given parameters are altered; the results also show that acceptable results may be obtained even when the theory is stretched beyond its reasonable limits.

Finally, the original numerical problem has been vastly simplified. The slow flow problem that must be solved is so much simpler than the full Navier–Stokes problem that three-dimensional time-dependent computations are a real possibility; in any case the theory generates a number of test cases that may be compared with numerical codes that may be developed.

Further extensions to the work presented above are left to the reader. Future projects could include:

- It was assumed above that all of the tests are carried out at a constant temperature. But there is also interest in the "unsteady" temperature problem where a paste sample is put in a hot oven and flows as it heats up. How would this change the full problem, and what simple cases could still be solved in closed form to provide test cases for the numerics?
- What happens for a cylindrical block of paste? Does the change to such a geometry alter the qualitative flow of the paste? (This might be possible since the sample now only has sharp-angled sides at its top and bottom.)
- Suppose that an "instant" test was required where the sample was given a impulse (hit with a hammer, for example). How would this change the full problem? Could this experimental methodology reasonably be expected to give accurate results more quickly than the standard tests?
- As discussed above, it is known that under some circumstances the paste "segregates" and may no longer be regarded as a uniform mixture of pitch and fines. Given an initial segregation distribution, how would the modelling be affected?

Acknowledgement

Thanks are due to Dr. Svenn-Anton Halvorsen (Elkem a/s, Kristiansand, Norway) who first brought this problem to our attention at the 1988 Study Group with Industry, Heriot-Watt University.

References

[1] Bergstrom, T., Cowley, S , Fowler, A. C. & Seward, P. E. (1989) Segregation of carbon paste in a smelting electrode. IMA J. Appl. Math. **43**, 83–99

[2] Fitt, A. D. & Aitchison, J. M. (1993) Determining the effective viscosity of a carbon paste used for continuous electrode smelting. Fluid Dynamics Res. **11**, 37–59.

[3] Fitt, A. D & Howell P D (1997) The manufacture of continuous smelting electrodes using carbon paste briquettes. J. Eng. Math. **33**, 353–376.

[4] Hinch, J (ed.) (1995) Temperature variations and control of a calciner, *Proc. 28th Study Group for Mathematics in Industry*, University of Cambridge, 1995.

[5] Moffatt, H. K. (1964) Viscous and resistive eddies near a sharp corner. J Fluid. Mech. **18**, 1–18.

[6] Nayfeh, A. H. (1973) *Perturbation Methods*, John Wiley & Sons.

[7] Ockendon, H. & Ockendon, J R. (1995) *Viscous Flow*, Cambridge University Press

[8] Penney, W. G & Thornhill, C. K. (1952) The dispersion, under gravity, of a column of fluid supported on a rigid, horizontal plane. Phil. Trans. Roy. Soc A **244**, 285–311

[9] Spence, D A. (1982) A note on the eigenfunction expansion for the elastic strip. SIAM J Appl Math. **42**, 155–173

Alistair D. Fitt
Faculty of Mathematical Studies, University of Southampton,
Southampton SO17 1BJ, UK
adf@maths. soton ac. uk